Water Air Soil Pollut (2013) 224:1582
DOI 10.1007/s11270-013-1582-5

Tobacco Stem Ash as an Adsorbent for Removal of Methylene Blue from Aqueous Solution: Equilibrium, Kinetics, and Mechanism of Adsorption

Rakesh Kumar Ghosh · D. Damodar Reddy

Received: 14 November 2012 / Accepted: 18 April 2013 / Published online: 5 May 2013

Abstract Tobacco (*Nicotiana tabacum L.*) stem ash (TSA) was evaluated as an adsorbent for removal of methylene blue (MB) from aqueous solution by batch adsorption method. MB adsorption increased with increase in contact time, initial solution pH, and adsorbent dose. Contact time for adsorption equilibrium was 180 min. The MB adsorption per unit mass of adsorbent (in milligram per gram) increased with the increasing initial dye concentration. Adsorption of MB onto TSA followed the pseudo-second-order kinetic model with a rate constant (k_2) of 0.017 g mg^{-1} min^{-1}. The mechanism of adsorption was described with intra-particle diffusion model. It was found that the intra-particle diffusion was not a sole rate-controlling step. Equilibrium adsorption was investigated by the Freundlich, Langmuir, Temkin, and Jovanoic isotherms. On the basis of coefficient of determination, the order of isotherm fit was Langmuir (R^2=0.974) > Freundlich (R^2=0.957) = Temkin (R^2=0.957) > Jovanoic (R^2=0.764) isotherm. The maximum monolayer adsorption capacity of TSA was 35.7 mg g^{-1}. The dimensionless separation factor (R_L) was low (0.137), indicating favorable adsorption of MB onto TSA. The results clearly demonstrate the potential of TSA as a low-cost and an easily available adsorbent for sequestering MB from wastewater.

R. K. Ghosh (✉) · D. D. Reddy
Division of Crop Chemistry and Soil Science, Central Tobacco Research Institute,
Rajahmundry 533105, Andhra Pradesh, India
e-mail: iarirakesh@gmail.com

Keywords Tobacco stem ash · Methylene blue removal · Adsorption kinetics · Isotherm models

1 Introduction

In the present era of industrialization and consumerism, the industries such as textile, rubber, paper, printing, leather, plastics, etc. use a wide variety of synthetic dyes to impart myriad color combinations to finished goods. About 5–10 % of dye stuffs used in these industries is, however, lost in the industrial wastewater (Dawood and Sen 2012). Discharge of untreated or partially treated dye-bearing industrial wastewater into environment poses a serious threat to life, not only by retarding the physicochemical and biological properties of environmental components but also from toxicological stand point (Montano et al. 2008; Abd EI-Latif et al. 2010) and, hence, is an environmental issue of serious concern. Therefore, removal of dye from wastewater is an essential prerequisite for environment-friendly disposal of dye-containing industrial effluents. In the recent past, several methods including adsorption, biosorption, biodegradation, electrochemical degradation, photochemical degradation, coagulation/flocculation, sonicated degradation, membrane filtration, etc. have been employed for the treatment of dye-containing wastewater (Feng et al. 2012; Somasekhara Reddy et al. 2012). Though every method has its own limitations in terms of situation suitability, applicability, and cost effectiveness, the adsorption method of dye removal is widely reported

to be very effective and practically feasible (Rafatullah et al. 2010; Salleh et al. 2011). Activated carbon is undoubtedly an excellent adsorbent for dye sequestration, but its high price limits its large-scale use. In the quest for low-cost, easily available, and effective adsorbents, several natural materials, wastes/by-products from agriculture or industries have been evaluated with variable degree of sources. Some of these biosorbents include saw dust of oak (Ferrero 2007), peel of banana (Annadurai et al. 2002), neem sawdust (Khattri and Singh 2000), beer brewery waste (Tsai et al. 2008) as by-products/wastes from agriculture/agro-industry, coir pith carbon (Kavitha and Namasivayam 2007), activated carbon from apricot and walnut shell (Aygun et al. 2003) as carbon/activated carbon-based adsorbents, and ash-based adsorbents include bagasse fly ash (Gupta et al. 2000), rice hull ash (Chen et al. 2012), rice husk ash (Sarkar and Bandyopadhyay 2010), fly ash (Wang et al. 2005), sonochemical treated fly ash (Wang and Zhu 2005), H_2SO_4-treated fly ash (Lin et al. 2008), bio-sludge ash (Weng and Pan 2006), *Salvadora persica* stem ash (Bazrafshan et al. 2012), etc. In this study, tobacco (*Nicotiana tabacum L.*) stem ash (TSA) has been evaluated for the removal of methylene blue (MB) from aqueous solution.

Tobacco, one of the world's leading nonfood cash crops, is grown extensively in countries such as India, China, Brazil, USA, etc. and generates huge quantity of stem biomass (1,000 kg ha^{-1}) as a primary byproduct in the production of tobacco leaf (economic part). The crop residues such as the tobacco stems left in the field generally pose hindrance to agro-machinery operations and harbor diseases/pests for subsequent crops (Lal 2005). Consequently, the common practice in vogue is to either burn such resides in situ or remove them from the field for use as firewood for domestic energy purposes or for thermal curing of tobacco leaf. Use of tobacco stems for fuel/thermal energy purposes (for curing tobacco leaf in curing barns) generates stem ash, a secondary byproduct with no known economic uses. The present study aims to evaluate TSA as an adsorbent to remove MB from aqueous solution. Effects of various factors including contact tine, initial solution pH, and adsorbent dose on MB adsorption has been examined to explore the MB adsorption behavior of TSA. Pseudo-first-order, pseudo-second-order, and intra-particle diffusion models were used to understand the kinetics and mechanism of adsorption. Four isotherm models, namely the Freundlich, Langmuir, Temkin, and Jovanoic isotherm were tested to understand nature of adsorption equilibrium. Dye adsorption capacity of TSA and feasibility of adsorption system were also investigated.

2 Materials and Methods

2.1 Reagents and Adsorbent

All chemicals used in this study were of analytical grade with high purity. Analytical grade MB (basic blue 9, molecular weight 373.91 g mol^{-1}) was procured from Qualigens®. Analytical-grade hydrochloric acid, nitric acid, potassium nitrate, potassium hydroxide, and sodium hydroxide were procured from SdFine®. MB stock solution (1,000 mg L^{-1}) was prepared by dissolving 1 g MB in 1 L of distilled water and subsequently diluted to achieve the required dye concentration for adsorption experiments. The pH of the MB solutions was 6.9. The MB concentration in aqueous solution was determined by using UV–VIS spectrophotometer at a wavelength of maximum absorbance (λ_{max}) at 665 nm. Preliminary studies with blank dye (MB) solution indicated that change of initial solution pH (pH 2.08 to 11) of dye solution had negligible effect on the λ_{max} (665 nm) of MB. This indicates the stability of the dye molecule within the studied range of pH. A similar kind of observation was reported by Gupta et al. (2000) for stability and λ_{max} of MB over a pH range from 2.00 to 10.00. Therefore, the calibration curve was used in all adsorption experiments prepared in distilled water at pH 6.9.

Tobacco (*N. tabacum L.*) stems were collected from experimental fields of the Central Tobacco Research Institute, Rajahmundry, Andhra Pradesh. Stem residues were cleaned thoroughly to remove the surface-adhered soil and then dried. The dried tobacco stems (5 kg) were burned in open air in a way much similar to the practice followed by the local tobacco farmers, i.e., burning of tobacco stems kept in heaps. Care was taken to ensure complete burning of the stem biomass, i.e., until no portion of the biomass remained unburned. The 5-kg tobacco stem biomass was reduced to 0.346 kg after burning (a weight loss of 93.08 %) and resulted in the ash accounting for 6.92 % of the original biomass burned. The TSA so generated was passed through a 1-mm sieve and stored in a plastic container until its use in the present study.

2.2 Characterization of TSA (Adsorbent)

The TSA was analyzed for organic carbon using a Total Organic Carbon analyzer (Elementar, Vario TOC Select, Germany), pH (Systronics, Model 361, India), and electrical conductivity (Elico, Model CM 82T, India). The surface property of TSA was determined by measuring a pH of zero point charge (pH_{zpc}) by potentiometric mass titration method (Fiol and Villaescusa 2009). Three doses of TSA (5, 7.5, and 10 g L^{-1}) were agitated with 50 mL 0.03 M KNO_3 solution in a set of 150 mL of Erlenmeyer flasks at 250 rpm for 24 h until the pH became constant. Then, 0.5 mL 1 M KOH solution was added before titration to deprotonate the adsorbent's surface. The suspension was titrated by adding a small volume of 0.1 M HNO_3 solution, and the pH was recorded after each addition until the pH of the suspension became constant. A similar procedure was followed for 50 mL 0.03 M KNO_3 blank solution (without adsorbent). The potentiometric curves were drawn by plotting suspension equilibrium pH values against the volume of 0.1 M HNO_3 added, and pH_{zpc} was determined from the intersection of the potentiometric curves with the blank. TSA was analyzed by the Bruker ALPHA, a Fourier transform infrared (FTIR) using attenuated total reflectance system to determine functional groups. The sample was scanned (resolution 4 cm^{-1}) in the region of 4,000–400 cm^{-1}. The specific surface area was calculated by the methylene blue adsorption method following the procedure outlined by Weng and Pan (2006) who also reported that the surface area of an adsorbent by this method was similar to that obtained by the BET method.

2.3 Batch Adsorption Studies

2.3.1 Kinetic Experiments

Adsorption kinetic was studied by batch method with known amount of TSA (0.1 g) and 10 mL MB solution of known concentration (50.4 mg L^{-1}) in a series of 150 mL of Erlenmeyer flasks. Kinetic experiments were carried out at the natural pH of dye solution. Flasks, containing reaction mixture, were agitated at 150 rpm by an orbital shaker (Rotary Flask Shaker, Optics Technology, India) over a time period of 300 min. Then, the sets of three flasks each were withdrawn from the shaker at different time intervals (15, 30, 45, 60, 120, 180, 240, and 300 min). The reaction mixtures were centrifuged at 8,000 rpm for 10 min, and the MB concentration in the supernatant was estimated by measuring the absorbance with a UV–VIS spectrophotometer at 665 nm against the standard calibration curve. The amount of dye adsorbed at time t, q_t (in milligram per gram), and dye adsorption percentage were calculated as follows:

$$q_t = (C_i - C_t)V/W \quad (1)$$

$$\%\ \text{Adsorption} = 100(C_i - C_t)/C_i \quad (2)$$

where C_i is the initial MB concentration in the solution (in milligrams per liter), C_t is the MB concentration in the solution at time t (in milligrams per liter), V is volume of the solution (in liters), and W is the amount of adsorbent added (in grams).

Separate batch adsorption experiments were carried out to investigate the effect of adsorbent dose and initial solution pH on MB adsorption. The effect of adsorbent dose was studied by equilibrating different quantities of TSA (0.5, 1.0, 2.0, 5.0, 10.0, and 15.0 g L^{-1}) with 10 mL of MB solution (concentration=50.4 mg L^{-1}, pH 6.9) for a period of 180 min. The effect of initial solution pH was investigated by agitating 0.1 g TSA with 10 mL MB solution (50.4 mg L^{-1}) of different pH (2.08, 4.08, 6.02, 6.9, and 7.93) for a period of 180 min. The pH of dye solution at a desired level was obtained by adding 0.1 M HCl or 0.1 M NaOH. The MB concentration in the equilibrium solution was determined as per the procedure detailed under kinetic study. All batch adsorption studies were carried out at room temperature (27±1 °C).

2.3.2 Adsorption Equilibrium Experiments

Adsorption equilibrium experiments were carried out by agitating 0.1 g of TSA with 50 mL MB solution of different initial dye concentrations (30.4, 50.4, 108.4, 160.2, 183.0, and 341.0 mg L^{-1}) in a set of 150 mL of Erlenmeyer flasks at 150 rpm over a time period of 180 min which was determined sufficient from the earlier explained kinetic study. Samples were centrifuged, and the MB concentrations in samples were estimated as per Section 2.3.1. The amount of dye

adsorbed (q_e) at equilibrium (in milligram per gram) was calculated as follows:

$$q_e = (C_i - C_e)V/W \quad (3)$$

where C_e is the MB concentration in the solution at equilibrium (in milligrams per liter).

All experiments were carried out in triplicate, and relative standard deviation was calculated. Only mean values are reported (with relative standard deviation <10 % for all measurements) for ease of presentation. Adsorbate and TSA blanks were carried out simultaneously for all treatments as control to monitor interference.

2.4 Adsorption Kinetics

The adsorption kinetics of MB by TSA was investigated by fitting the kinetic data to popularly used mathematical models, namely pseudo-first-order, pseudo-second-order, and intra-particle diffusion models.

2.4.1 Pseudo-First-Order Model

The pseudo-first-order kinetic model, which has been popularly used for determination of adsorption rate based on the adsorption capacity, can be expressed in linear form (Somasekhara Reddy et al. 2012; Zhang et al. 2012; Feng et al. 2012) as follows:

$$\log(q_e - q_t) = \log\ q_e - (k_1/2.303)\ t \quad (4)$$

where q_e and q_t are the amount of dye adsorbed (in milligrams per gram) at equilibrium and time t (in minute), respectively, and k_1 is the rate constant for the pseudo-first-order model (per minute). The pseudo-first-order rate constant, k_1, can be calculated from the slope of the linear plot of log (q_e−q_t) against t.

2.4.2 Pseudo-Second-Order Model

The pseudo-second-order kinetic model, which is based on the assumption of chemisorptions by the interaction between polar functional groups on the sorbent surface and dyes, can be expressed in linear form (Somasekhara Reddy et al. 2012; Zhang et al. 2012; Feng et al. 2012) as follows:

$$t/q_t = 1/\left(k_2 q_e^2\right) + (1/q_e)\ t \quad (5)$$

where k_2 is the pseudo-second-order rate constant (in grams per milligram minute). q_e and k_2 can be calculated from the slope and intercept of the linear plot of t/q_t against t.

2.4.3 Intra-Particle Diffusion Model

Determination of the adsorption mechanism and particularly the rate-limiting stage has always been a point of interest in adsorption kinetic studies to gain details of the mechanism involved. To investigate the mechanism involved in MB sorption onto TSA, kinetic data were fitted to the widely used of intra-particle diffusion model, which can be expressed in linear form (Dawood and Sen 2012; Somasekhara Reddy et al. 2012; Yagub et al. 2012; Sen et al. 2011) as follows:

$$q_t = k_{id} t^{0.5} + C \quad (6)$$

where q_t is the amount adsorbed at time t, $t^{0.5}$ is the square root of the time, k_{id} (in milligrams per gram minute$^{0.5}$) is the rate constant of intra-particle diffusion, and C reflects the boundary layer effect. The k_{id} and C can be determined from the slope and intercept of the linear plot of q_t against $t^{0.5}$.

2.5 Adsorption Isotherm

The adsorption equilibrium data were tested by four isotherm models, namely the Freundlich, Langmuir, Temkin, and Jovanoic isotherm.

Freundlich Isotherm The empirical Freundlich isotherm (Freundlich 1906), which assumes sorption onto a heterogeneous surface, can be represented in a linear form as follows:

$$\log q_e = \log\ K_f + (1/n)\ \log\ C_e \quad (7)$$

where q_e is the amount of dye adsorbed at equilibrium (in milligrams per gram), and C_e is the dye concentration in solution at equilibrium (in milligrams per liter). K_f and $1/n$ are Freundlich constants which indicate capacity and heterogeneity factor. The value of $1/n$ ranged from 0 to 1, and $1/n$ value closer to 1 indicates high surface heterogeneity. The K_f and $1/n$ can be calculated from the intercept and slope of the linear plot of log q_e against log C_e.

Langmuir Isotherm The Langmuir isotherm (Langmuir 1918), which assumes monolayer adsorption onto a homogeneous surface with a finite number of identical adsorption sites, can be represented in a linear form as follows:

$$C_e/q_e = 1/kb + C_e/b \quad (8)$$

where b is the maximum adsorption capacity, called Langmuir maxima constant (in milligrams per gram), and k (in liters per milligram) is the Langmuir bonding energy coefficient. The k and b can be calculated from the intercept and slope of the linear plot of C_e/q_e against C_e.

Temkin Isotherm The Temkin isotherm (Temkin and Pyzhev 1940), which assumes that the heat of adsorption of all the molecules in the layer decreases linearly with coverage due to adsorbent–adsorbate interactions and characterized by a uniform distribution of binding energies up to some maximum binding energy, can be represented in a linear form as follows:

$$q_e = \alpha + \beta\ lnC_e \quad (9)$$

where α and β are constants, representing adsorption capacity and retention intensity of adsorption. The α and β can be calculated from the intercept and slope of the linear plot of q_e against lnC_e.

Jovanoic Isotherm The Jovanoic isotherm (Jovanovic 1969), which is based on the same assumptions of the Langmuir isotherm, also considers the possibility of some mechanical contacts between the adsorbing and desorbing molecules on the homogeneous surface and can be represented in a linear form as follows:

$$lnq_e = lnq_m + K_J C_e \quad (10)$$

where q_m is the maximum amount adsorbed (in milligrams per gram) and K_J (in liters per milligram) is the constant related to the energy of adsorption. The q_m and K_J can be calculated from the intercept and slope of the linear plot of lnq_e against C_e.

3 Results and Discussion

3.1 Physicochemical Properties of the Adsorbent (TSA)

Physicochemical analysis showed that TSA contained 6.68 % organic carbon. The electrical conductivity of TSA was 7.1 dSm^{-1}, and pH was 11.16. The pHzpc of TSA was investigated to understand the adsorbent's surface charge property (Fig. 1). The pH_{zpc} of TSA was 10.38. The nature of functional groups present in the adsorbent's surface is of immense importance to understand the adsorption process. The FTIR spectroscopy has been widely used to characterize functional groups present in various adsorbents (Gupta et al. 2000; Hameed et al. 2008; Yagub et al. 2012). Figure 2 shows the FTIR spectrum of TSA. The FTIR spectrum shows several peaks indicating the presence of various functional groups which can help to understand the MB adsorption process. The peak at 1,045 cm^{-1} represents Si-O asymmetric stretching, and peaks in 700–800 cm^{-1} correspond to Si-O symmetric vibrations. Peaks in the area 500–650 cm^{-1} indicate silicate backbone of TSA. Peaks observed at 873 and 1,440 cm^{-1} represent out-of-plane bending vibration of carbonate (CO_3^{2-}) and asymmetric stretching vibration of carbonate (CO_3^{2-}). Similar peaks were observed in rice husk ash (Bhavornthanayod and Rungrojchaipon 2009), bagasse fly ash (Gupta et al. 2000), and fly ash (Sarkar et al. 2006). The specific surface area of TSA was 40.01 $m^2\ g^{-1}$.

3.2 Effect of Contact Time on MB Adsorption by TSA

The effect of contact time on MB adsorption was investigated at a fixed adsorbent dose with MB

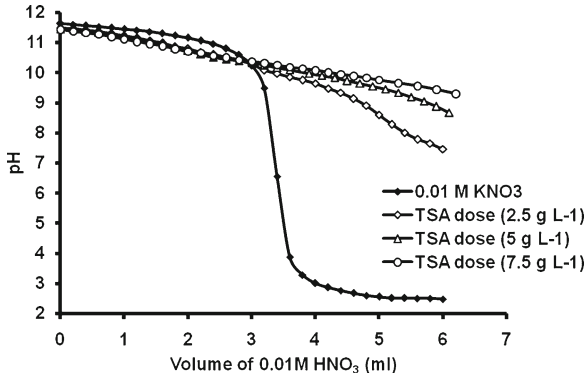

Fig. 1 Zero point charge determination of tobacco stem ash

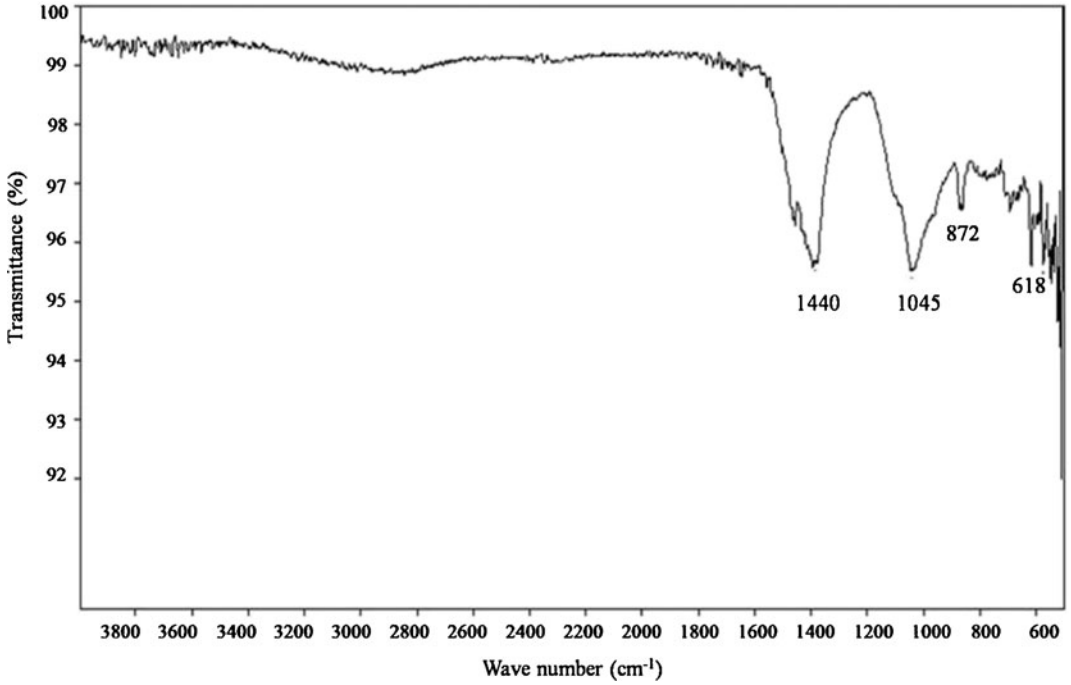

Fig. 2 FTIR spectra of tobacco stem ash

solution of known initial dye concentration, and results are depicted in Fig. 3. It shows that MB removal was fast in the initial stage of adsorption process, and nearly 48 % MB is sequestered within initial 15 min of adsorption. In the beginning, the adsorption sites of adsorbent were vacant. The moment they come in contact with dye molecules, adsorption of MB initiates with a fast rate as a result of diffusion process from the bulk solution to the sites (Yagub et al. 2012). However, the rate of adsorption decreased gradually with increase in contact time, leading to the state of equilibrium. It is very clear in Fig. 3 that adsorption increased up to 120 min, and thereafter, increase in MB adsorption was very less. Thus, in order to ensure the state of equilibrium for MB adsorption, 180 min was fixed as the time of equilibrium.

3.3 Effect of Adsorbent Dose on MB Adsorption by TSA

Evaluating the effect of adsorbent dose gives a dual idea about the effectiveness of an adsorbent and the minimum dose of adsorbent to remove dye most economically (Salleh et al. 2011). Figure 4 represents the effect of adsorbent (TSA) dose on MB sequestration from a fixed volume of MB solution of known initial concentration (50.4 mg L^{-1}). Percentage MB adsorption increased from 18 to 75 % with increase in the adsorbent dose from 0.5 to 10 g L^{-1} (Fig. 4), and thereafter, it showed not much change. A TSA dose of 10 g L^{-1} was, therefore, used in other batch adsorption studies. At a fixed volume of known initial dye concentration, the adsorbent dose is of prime importance because a fixed amount of adsorbent has fixed adsorption sites. Thus, it can absorb only a fixed amount of dye from the dye solution. With

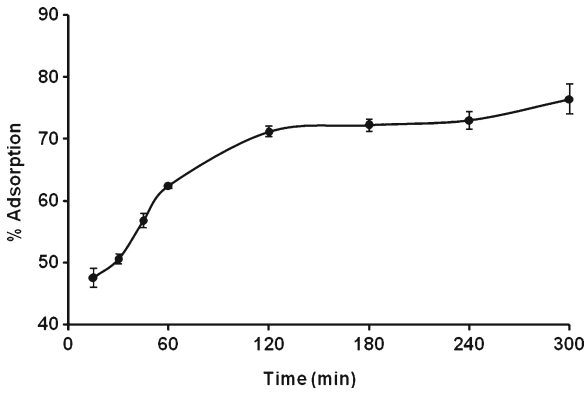

Fig. 3 Effect of contact time on MB adsorption onto tobacco stem ash; volume of dye solution=10 mL, initial dye concentration=50.4 mg L^{-1}, temperature=27±1 °C, shaker speed=150 rpm, tobacco stem ash dosage=0.1 g, initial solution pH=6.9

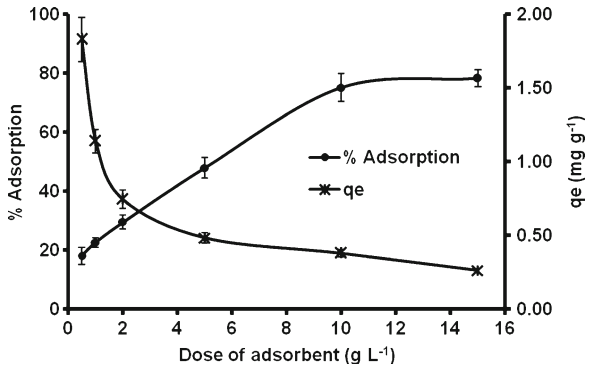

Fig. 4 Effect of adsorbent (tobacco stem ash) dose on the adsorption of MB; initial dye concentration=50.4 mg L^{-1}, temperature=27±1 °C, shaker speed=150 rpm, initial solution pH=6.9

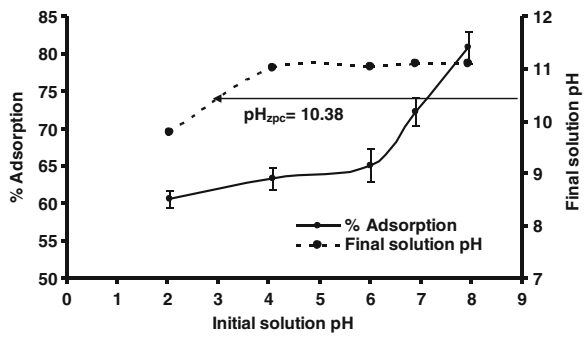

Fig. 5 Effect of initial solution pH on MB adsorption onto tobacco stem ash; volume of dye solution=10 mL, initial dye concentration=50.4 mg L^{-1}, temperature=27±1 °C, shaker speed=150 rpm, tobacco stem ash dosage=0.1 g

increase in the adsorbent dose, the number of adsorption sites increases, and consequently, more dye molecules get adsorbed. However, q_e (in milligram per gram) decreased from 1.83 to 0.38 mg g^{-1} with increase in the dose of adsorbent from 0.5 to 10 g L^{-1}. This could be because of the split in the flux or the concentration gradient between solute concentration in the solution and the solute concentration on the surface of the adsorbent (Sen et al. 2011; Vadivelan and Kumar 2005). The pH of MB solution increased from its initial value of 6.90 to 10.66, 10.71, 10.90, 10.95, 11.10, and 11.17 due to the addition of adsorbent at 0.5, 1.0, 2.0, 5.0, 10.0, and 15.0 g L^{-1}, respectively. The rise in the pH of the final solution with increase in adsorbent dose may be attributed to the fact that increase in negatively charged sites with increasing adsorbent dose can induce adsorption of more H^+ ions, thus resulting in an increase of solution pH (Arias and Sen 2009; Yagub et al. 2012). Similar observations were reported for MB adsorption on pine cone biomass (Sen et al. 2011), cypress cone chips (Fernandez et al. 2010), sugarcane bagasse (Sharma and Kaur 2011), and papaya leaf powder (Mukhlish et al. 2012).

3.4 Effect of Initial Solution pH on MB Adsorption by TSA

The initial dye solution pH is a very important factor which affects the dye removal efficiency of any adsorbent by influencing the degree of ionization of dye molecules and the surface properties of adsorbent (Yagub et al. 2012; Sen et al. 2011; Somasekhara Reddy et al. 2012). The initial solution pH as a factor influencing MB adsorption onto TSA was studied by varying pH of dye-containing solution. Figure 5 depicts the changes in the percentage MB adsorption for a fixed dose of adsorbent at varying initial pH of dye solution. The percentage MB adsorption increased from 60 to 81 % due to an increase in the initial dye solution pH from 2.08 to 7.93, with the magnitude of increase being larger at neutral to alkaline pH range. The MB, being a cationic dye, gets adsorbed onto the negatively charged adsorption sites of the adsorbent as a result of electrostatic attraction. Relatively low adsorption of MB at the strongly acidic pH (2.08) can be attributed partly to the competition between H^+ ions and cationic MB molecules for the same adsorption sites, and partly to a decrease in the negative charge density on the adsorption sites owing to protonation of the adsorbent's surface. In contrast, the increased MB adsorption at the initial solution pH of 4.08 and above may be ascribed to a sharp rise in the solution pH beyond pH_{zpc} of the adsorbent (10.38) as evidenced from the final solution pH (Fig. 5). With the solution pH values above pH_{zpc} of adsorbent, the negative charge density on the adsorbent surface increased and consequently resulted in greater adsorption of cationic MB. Similar observations were reported for MB adsorption on rice husk (Vadivelan and Kumar 2005), on pine tree leaf (Yagub et al. 2012), on sludge ash (Weng and Pan 2006), and on *S. persica* stem ash (Bazrafshan et al. 2012).

3.5 Adsorption Kinetics

The pseudo-first-order and pseudo-second-order models were used to understand the kinetic nature of TSA-MB sorption system. The value of pseudo-first-order rate constant (k_1) and amount adsorbed at equilibrium (q_e) were calculated and presented in Table 1. The experimental q_e value is not in agreement with the

Table 1 Comparison of the pseudo-first-order, pseudo-second-order, and intra-particle diffusion model parameters for methylene blue adsorption onto tobacco stem ash (TSA)

Mathematical models	Parameters	Values
Pseudo-first-order kinetic model		
	k_1 (min^{-1})	0.029
	q_e (mg g^{-1}) calculated	2.67
	q_e (mg g^{-1}) experimental	3.61
	R^2	0.971
Pseudo-second-order kinetic model		
	k_2 (g mg^{-1} min^{-1})	0.017
	q_e (mg g^{-1}) calculated	3.95
	q_e (mg g^{-1}) experimental	3.61
	R^2	0.998
Intra-particle diffusion model		
	K_{id}	0.141
	C	1.878
	R^2	0.937

calculated q_e value from the pseudo-first-order model, though the coefficient of determination value is more than 0.97. These results suggest that the pseudo-first-order kinetic model is not appropriate in describing MB sequestration onto TSA. The pseudo-second-order rate constant, k_2, and amount adsorbed at equilibrium (q_e) were calculated from the slope and intercept of the linear plot of t/q_t against t (Fig. 6), and values are shown in Table 1. The experimental q_e value is in close agreement with the calculated q_e value from the pseudo-second-order kinetic model, with corresponding very high coefficient of determination (>0.99). It suggests that MB adsorption kinetics onto TSA is better explained by the pseudo-second-order model. The value of pseudo-second-order rate constant, k_2, for MB-TSA system is 0.017 g mg^{-1} min^{-1} which is in agreement with the values reported earlier for some MB biosorbents (Vadivelan and Kumar 2005; Fernandez et al. 2010; Sen et al. 2011).

3.5.1 Adsorption Mechanism

Identification of the rate-controlling stage has always been a point of interest to understand the mechanism of adsorption. Reported literature shows that transfer of the dye molecules from the bulk solution to the adsorbent surface is either through external mass transfer (boundary layer diffusion) or intra-particle diffusion or both (Dawood and Sen 2012; Yagub et al. 2012). To investigate the mechanism involved in MB sorption onto TSA, kinetic data were fitted to the intra-particle diffusion model as per Eq. (6). The plot of q_t against $t^{0.5}$ is shown in Fig. 7. It is very clear that adsorption plots are not linear over the whole time frame and can be separated into multilinear regions which confirm the multistages of adsorption (Kavitha and Namasivayam 2007). The intra-particle diffusion rate constant (k_{id}) and C which indicate the boundary layer effect can be determined from the slope and intercept of the linear regression lines. The k_{id} and C values are presented in Table 1. If the linear regression of q_t versus $t^{0.5}$ passes through the origin (C=0), then intra-particle diffusion is the sole rate-controlling step.

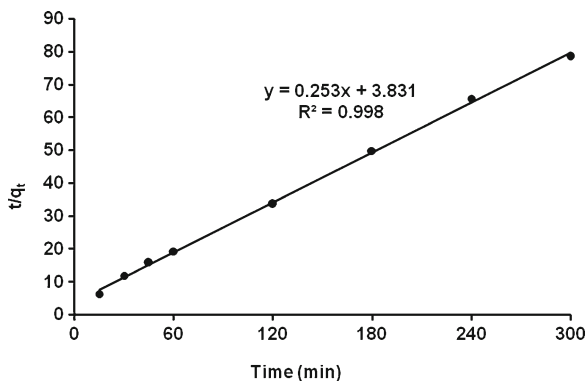

Fig. 6 Pseudo-second-order kinetic model for MB adsorption onto tobacco stem ash; volume of dye solution=10 mL, initial dye concentration=50.4 mg L^{-1}, temperature=27±1 °C, shaker speed=150 rpm, tobacco stem ash dosage=0.1 g, initial solution pH=6.9

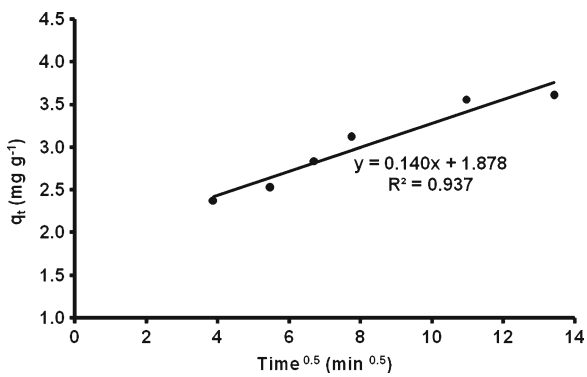

Fig. 7 Intra-particle diffusion model for MB adsorption onto tobacco stem ash; volume of dye solution=10 mL, initial dye concentration=50.4 mg L^{-1}, temperature=27±1 °C, shaker speed=150 rpm, tobacco stem ash dosage=0.1 g, initial solution pH=6.9

Figure 5 and Table 1 clearly show that the regression line does not pass through origin and $C \neq 0$. Thus, intra-particle diffusion is not the only rate-controlling step, and this finding is in agreement with some earlier reports (Zhang et al. 2012; Sen et al. 2011). According to the reported literature, fast adsorption in the initial stage can be controlled by boundary layer and intra-particle diffusion, while at the later stage, the slow adsorption can be governed by intra-particle diffusion (Marungrueng and Pavasant 2007).

3.6 Adsorption Isotherm

Adsorption equilibrium experiment indicates the adsorbate–adsorbent interaction and adsorption capacity of adsorbent. Equilibrium is attained when the amount of dye being adsorbed onto adsorbent is equal to the amount being desorbed, and at that point, equilibrium solution concentration remains constant. Figure 8 clearly shows that, for a fixed dose of adsorbent at equilibrium, the amount of dye adsorbed (q_e) on TSA increases with increase in initial dye concentration (C_i), while the percentage MB adsorption decreases. The reason is that, with increase in the initial dye concentration, the driving force for dye transfer from the solution to the adsorbent increases and results in higher q_e values. However, with increase in the initial dye concentration, most of the adsorption sites of adsorbent become occupied, and availability of adsorption sites becomes limited which results in a decrease in percent dye adsorption. This indicates a monolayer nature of MB adsorption onto TSA. To understand the adsorption equilibrium behavior, four isotherms, namely the Freundlich, Langmuir, Temkin, and Jovanoic isotherm models were tested, and Table 2 summarizes the isotherm parameter values. The best fitted model is selected on the basis of coefficient of determination values, and the order of isotherms is Langmuir (R^2=0.974) > Freundlich (R^2=0.957) = Temkin (R^2=0.957) > Jovanoic (R^2=0.764) isotherm. The best-fit Langmuir isotherm can be drawn by plotting C_e/q_e against C_e (Fig. 9). According to the Langmuir isotherm, the maximum monolayer adsorption capacity (b) of TSA for MB was 35.7 mg g^{-1}. Further, the essential characteristic of the Langmuir isotherm can be expressed in terms of a widely used dimensionless factor called equilibrium parameter (R_L), also known as the separation factor (Sen et al. 2011; Somasekhara Reddy et al. 2012). The R_L factor can be calculated by the following expression:

$$R_L = 1/(1 + kC_i) \quad (11)$$

where k (in liters per milligram) is the Langmuir bonding energy coefficient, and C_i is the highest initial dye concentration (in milligrams per liter). The value of R_L indicates the feasibility of dye adsorption. The value of

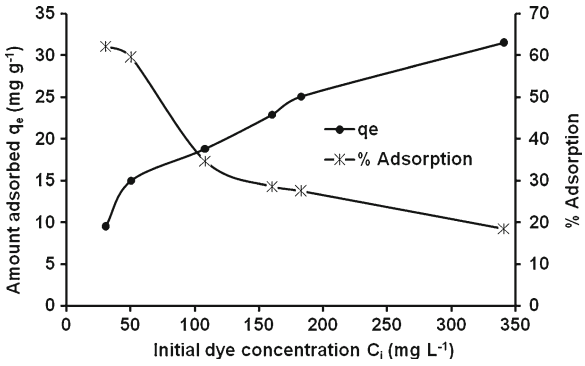

Fig. 8 Effect of initial dye concentration on MB adsorption onto tobacco stem ash: volume of dye solution=50 mL; initial dye concentration C_i=30.4, 50.4, 108.4, 160.2, 183.0, and 341.0 mg L^{-1}; temperature=27±1 °C; shaker speed=150 rpm; tobacco stem ash dosage=0.1 g; initial solution pH=6.9

Table 2 Different adsorption isotherm model parameters for the adsorption of methylene blue onto tobacco stem ash (TSA)

Mathematical models	Parameters	Values
Freundlich isotherm		
	K_f	4.52
	$1/n$	0.345
	R^2	0.957
Langmuir isotherm		
	b (mg g^{-1})	35.7
	k (L mg^{-1})	0.023
	R_L	0.111
	R^2	0.974
Temkin isotherm		
	α	5.8
	β	6.31
	R^2	0.957
Jovanoic isotherm		
	q (mg g^{-1})	12.8
	K_j (L mg^{-1})	0.003
	R^2	0.764

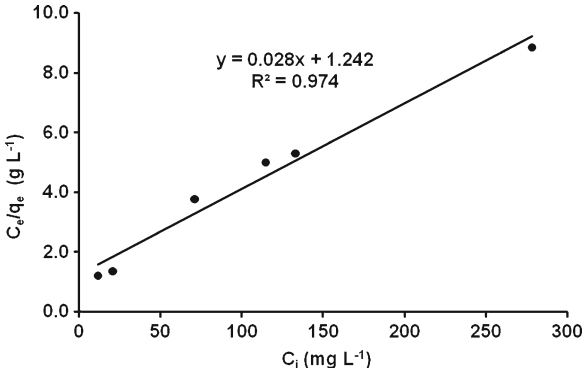

Fig. 9 Langmuir equilibrium isotherm for MB adsorption onto tobacco stem ash: volume of dye solution=50 mL; initial dye concentration C_i=30.4, 50.4, 108.4, 160.2, 183.0, and 341.0 mg L^{-1}; temperature=27±1 °C; shaker speed=150 rpm; tobacco stem ash dosage=0.1 g; initial solution pH=6.9

R_L indicates either unfavorable (R_L>1), linear (R_L=1), favorable (0<R_L<1), or irreversible (R_L=0) adsorption system. The R_L value at the highest initial dye concentration has been calculated from the Langmuir isotherm, and the value is 0.137 which indicates a favorable (0<R_L<1) system of adsorption.

3.6.1 Comparison of TSA with Some Previously Reported Low-Cost Adsorbents

Table 3 represents a comparative evaluation among some previously reported low-cost adsorbents including agriculture/agro-industrial byproduct, carbon/activated carbon products, and ash-based adsorbents with the studied TSA. The MB removal capacity of TSA is found substantially superior than that of many reported low-cost adsorbents. Therefore, TSA emerges as a potential adsorbent to sequester MB from aqueous solutions.

4 Conclusion

The present study reveals that TSA is effective in MB sequestration from aqueous solution. The equilibrium contact time is 180 min. MB adsorption onto TSA is pH-dependent, and adsorption increased with an increase in the initial solution pH. The percentage MB adsorption increases with an increase in adsorbent dose, while showing a decrease with increasing initial dye concentration. Adsorption kinetics is of pseudo-

Table 3 Comparison of methylene blue adsorption capacities of different absorbents

Adsorbents	pH	Contact time	Adsorption capacity (mg g^{-1})	Reference
Agriculture/ agro-industrial by-products				
Banana peel	7.2	24 h	20.8	Annadurai et al. 2002
Saw dust of oak	–	180 min	29.94	Ferrero 2007
Neem sawdust	7.2	30 min	3.62	Khattri and Singh 2000
Beer brewery waste	7.0	24 h	4.92	Tsai et al. 2008
Carbon/activated carbons				
Coir pith carbon	6.9	100 min	5.87	Kavitha and Namasivayam 2007
Apricot shell activated carbon 750 °C	7.0	24 h	4.11	Aygun et al. 2003
Walnut shell activated carbon 750 °C	7.0	24 h	3.53	Aygun et al. 2003
Ash-based products				
Bagasse fly ash	8.0	24 h	75.53	Gupta et al. 2000
Rice hull ash	–	150 min	50.51	Chen et al. 2012
Rice husk ash	7.2	60 min	6.9	Sarkar and Bandyopadhyay 2010
Fly ash	–	100 h	6.40	Wang et al. 2005
Fly ash (sonochemically treated)	9.4	–	4.48	Wang and Zhu 2005
Fly ash (H_2SO_4 treated)	–	72 h	0.785	Lin et al. 2008
Bio-sludge ash	9.83	72 h	1.87	Weng and Pan 2006
Salvadora persica stem ash	11.0	80 min	22.78	Bazrafshan et al. 2012
Tobacco stem ash (TSA)	6.9	180 min	35.7	Present study

second-order nature. Intra-particle diffusion is not the sole rate-controlling step. The Langmiur isotherm is the best-fit model for the adsorption equilibrium, as compared to the Freundlich, Temkin, and Jovanoic isotherm. The maximum monolayer adsorption capacity is 35.7 mg g^{-1}. The dimensionless separation factor (R_L) indicates a favorable system for MB adsorption onto TSA. This study demonstrates that TSA is a potential adsorbent for MB and could be used as an efficient, low-cost, and easily available adsorbent for the treatment of dye-containing industrial wastewater.

Acknowledgments The authors wish to thank the Director, C.T.R.I., for extending all facilities required for this research, and M. K. Rupnath, Mrs. N. Ramalakshmi, and the technical staff of CC and SS Division, C.T.R.I., for their assistance throughout the course of this study.

References

Abd EI-Latif, M. M., Ibrahim, A. M., & EI-Kady, M. F. (2010). Adsorption equilibrium, kinetics and thermodynamics of methylene blue from aqueous solutions using biopolymer oak sawdust composite. *Journal of American Science, 6*(6), 267–283.

Annadurai, G., Juang, R., & Lee, D. (2002). Use of cellulose based wastes for adsorption of dyes from aqueous solutions. *Journal of Hazardous Materials, B92*(3), 263–274.

Arias, F., & Sen, T. K. (2009). Removal of zinc metal ion (Zn2+) from its aqueous solution by kaolin clay mineral: a kinetic and equilibrium study. *Colloids and Surfaces A: Physicochemical and Engineering Aspects, 348*, 100–108.

Aygun, A., Yenisoy-Karakas, S., & Duman, I. (2003). Production of granular activated carbon from fruit stones and nutshells and evaluation of their physical, chemical and adsorption properties. *Microporous Mesoporous Material, 66*(2–3), 189–195.

Bazrafshan, E., Mostafapour, F., & Zazouli, M. A. (2012). Methylene blue (cationic dye) adsorption into *Salvadora persica* stems ash. *African Journal of Biotechnology, 11* (101), 16661–16668.

Bhavornthanayod, C., & Rungrojchaipon, P. (2009). Synthesis of zeolite a membrane from rice husk ash. *Journal of Metals, Materials and Minerals, 19*(2), 79–83.

Chen, X. G., Lv, S. S., Liu, S. T., Zhang, P. P., Zhang, A. B., Sun, J., et al. (2012). Adsorption of methylene blue by rice hull ash. *Separation Science and Technology, 47*(1), 147–156.

Dawood, S., & Sen, T. K. (2012). Removal of anionic dye Congo red from aqueous solution by raw pine and acid-treated pine cone powder as adsorbent: Equilibrium, thermodynamic, kinetics, mechanism and process design. *Water Research, 46*(6), 1933–1946.

Feng, Y., Zhou, H., Liu, G., Qiao, J., Wanga, J., Lu, H., et al. (2012). Methylene blue adsorption onto swede rape straw (*Brassica napus L.*) modified by tartaric acid: Equilibrium, kinetic and adsorption mechanisms. *Bioresource Technology, 125*, 138–144.

Fernandez, M. E., Nunell, G. V., Bonelli, P. R., & Cukierman, A. L. (2010). Effectiveness of *Cupressus sempervirens* cones as biosorbent for the removal of basic dyes from aqueous solutions in batch and dynamic modes. *Bioresource Technology, 101*(24), 9500–9507.

Ferrero, F. (2007). Dye removal by low cost adsorbents: Hazelnut shells in comparison with wood sawdust. *Journal of Hazardous Materials, 142*(1–2), 144–152.

Fiol, N., & Villaescusa, I. (2009). Determination of sorbent point zero charge: usefulness in sorption studies. *Environmental Chemistry Letters, 7*(1), 79–84.

Freundlich, H. (1906). Adsorption in solution. *Physical Chemical Society, 40*, 1361–1368.

Gupta, V. K., Mohan, D., Sharma, S., & Sharma, M. (2000). Removal of basic dyes (Rhodamine B and Methylene Blue) from aqueous solutions using bagasse fly ash. *Separation Science and Technology, 35*(13), 2097–2113.

Hameed, B. H., Mahmoud, D. K., & Ahmad, A. L. (2008). Equilibrium modeling and kinetic studies on the adsorption of basic dye by a low-cost adsorbent: Coconut (*Cocos nucifera*) bunch waste. *Journal of Hazardous Materials, 158*, 65–72.

Jovanovic, D. S. (1969). Physical adsorption of gases I: Isotherms for monolayer and multilayer adsorption. *Colloid & Polymer Science, 235*, 1203–1214.

Kavitha, D., & Namasivayam, C. (2007). Experimental and kinetic studies on methylene blue adsorption by coir pith carbon. *Bioresource Technology, 98*(1), 14–21.

Khattri, S. D., & Singh, M. K. (2000). Colour removal from synthetic dye wastewater using a bioadsorbent. *Water, Air, and Soil Pollution, 120*, 283–294.

Lal, R. (2005). World crop residues production and implications of its use as a biofuel. *Environment International, 31*(4), 575–584.

Langmuir, I. (1918). The adsorption of gases on plane surfaces of glass, mica, and platinum. *Journal of the American Chemical Society, 40*, 1361–1368.

Lin, J. X., Zhan, S. L., Fang, M. H., Qian, X. Q., & Yang, H. (2008). Adsorption of basic dye from aqueous solution onto fly ash. *Journal of Hazardous Materials, 87*(1), 193–200.

Marungrueng, K., & Pavasant, P. (2007). High performance biosorbent (*Caulerpa lentillifera*) for basic dye removal. *Bioresource Technology, 98*(8), 1567–1572.

Montano, J. G., Torrades, F., Perez Estrada, L. A., Oller, I., Malato, S., Maldonado, M. I., et al. (2008). Degradation pathways of the commercial reactive azo dye Procion Red H-E7B under solar-assisted photo-Fenton reaction. *Environmental Science and Technology, 42*(17), 6663–6670.

Mukhlish, M. Z. B., Khan, M. R., Bhoumick, M. C., & Paul, S. (2012). Papaya (*Carica papaya L.*) leaf powder: Novel adsorbent for removal of methylene blue from aqueous solution. *Water, Air, and Soil Pollution, 223*(8), 4949–4958.

Rafatullah, M., Sulaiman, O., Hashim, R., & Ahmad, A. (2010). Adsorption of methylene blue on low-cost adsorbents; a review. *Journal of Hazardous Materials, 177*, 70–80.

Salleh, M. A. M., Mahmoud, D. K., Karim, W. A., & Idris, A. (2011). Cationic and anionic dye adsorption by agricultural solid wastes: A comprehensive review. *Desalination, 280*(1–3), 1–13.

Sarkar, A., Rano, R., Udaybhanu, G., & Basu, A. K. (2006). A comprehensive characterization of fly ash from a thermal power plant in Eastern India. *Fuel Processing Technology, 87*, 259–277.

Sarkar, D., & Bandyopadhyay, A. (2010). Adsorptive mass transport of dye on rice husk ash. *Journal of Water Resource and Protection, 2*, 424–431.

Sen, T. K., Afroze, S., & Ang, H. (2011). Equilibrium, kinetics and mechanism of removal of methylene blue from aqueous solution by adsorption onto pine cone biomass of *Pinus radiata*. *Water, Air, and Soil Pollution, 218*(1–4), 499–515.

Sharma, P., & Kaur, H. (2011). Sugarcane bagasse for the removal of erythrosin B and methylene blue from aqueous waste. *Applied Water Science, 1*(3–4), 135–145.

Somasekhara Reddy, M. C., Sivaramakrishna, L., & Varada Reddy, A. (2012). The use of an agricultural waste material, Jujuba seeds for the removal of anionic dye (Congo red) from aqueous medium. *Journal of Hazardous Materials, 203–204*, 118–127.

Temkin, M. J., & Pyzhev, V. (1940). Kinetics of ammonia synthesis on promoted iron catalysts. *Acta Physiochim URSS, 12*, 217–222.

Tsai, W. T., Hsu, H. C., Su, T. Y., Lin, K. Y., & Lin, C. M. (2008). Removal of basic dye (methylene blue) from wastewaters utilizing beer brewery waste. *Journal of Hazardous Materials, 154*(1–3), 73–78.

Vadivelan, V., & Kumar, K. V. (2005). Equilibrium, kinetics, mechanism, and process design for the sorption of methylene blue onto rice husk. *Journal of Colloid and Interface Science, 286*(1), 90–100.

Wang, S., & Zhu, Z. H. (2005). Sonochemical treatment of fly ash for dye removal from wastewater. *Journal of Hazardous Materials, 126*(1–3), 91–95.

Wang, S., Boyjoo, Y., & Choueib, A. (2005). A comparative study of dye removal using fly ash treated by different methods. *Chemosphere, 60*(10), 1401–1407.

Weng, C. H., & Pan, Y. F. (2006). Adsorption characteristics of methylene blue from aqueous solution by sludge ash. *Colloids and Surfaces A: Physicochemical and Engineering Aspects, 274*(1), 154–162.

Yagub, M. T., Sen, T. K., & Ang, H. M. (2012). Equilibrium, kinetics, and thermodynamics of methylene blue adsorption by pine tree leaves. *Water, Air, and Soil Pollution, 223*(8), 5267–5282.

Zhang, W., Li, H., Kan, X., Dong, L., Yan, H., Jiang, Z., et al. (2012). Adsorption of anionic dyes from aqueous solutions using chemically modified straw. *Bioresource Technology, 117*, 40–47.